Reliability Analysis of a Switched Reluctance Starter/Generator

Hao Chen, Fan Yang, Lijun Xu, Qiwei Lu, Xiqiang Chang, Xing Wang, Lijiang Dong, Yi Wen, Jiang Chen, Gang Miao, Jianmin Hu, Guanjun Wang, Wei Li, and Xiaohua Bao

***Abstract*—In this paper, the combined *k*-out-of-*n*:G model and reliability block diagram model is used to analyze the reliability of a switched reluctance starter/generator system. First, the different operational modes of a switched reluctance motor starter/generator are analyzed, and the fault states of the system are briefly described. Then the fault criteria of the system in different operational states are put forward. Secondly, a reliability block diagram model is established to calculate the system-level reliability, and the *k*-out-of-*n*:G model is adopted to analyze the reliability of each part of the switched reluctance starter/generator system. To verify effectiveness, the first-order Markov model is also used to analyze the reliability of each part of the switched reluctance starter/generator system. Considering the computational complexity and accuracy of the system, the *k*-out-of-*n*:G model is more suitable for system component level reliability analysis. Finally, a 6/4 switched reluctance motor is used as the simulated and experimental platform motor. The final results verify the effectiveness of the reliability analysis model.**

***Index Terms*—Switched reluctance motor, starter/generator, fault criterion, reliability block diagram, Markov model, *k*-out-of-*n*: G model.**

I. Introduction

With an increasing shortage of energy, green energy (such as wind, ocean wave and solar energy, etc.) has received ever increasing attention [1], [2]. Energy storage technology is an indispensable supporting technology in the development of renewable energy, the smart grid, distributed generation, electric vehicles and other fields. A flywheel battery (also known as flywheel energy storage) uses the acceleration and deceleration of a high-speed flywheel to realize the mutual conversion between electrical and mechanical energy. It can effectively increase the stability of the new energy grid. It is a clean and pollution-free energy storage method, and is finding new focus in recent years [3]–[6]. At present, the following types of motors are commonly used for flywheel motors: induction, permanent magnet and switched reluctance motors (SRM), etc. SRM is widely used in flywheel energy storage because of its simple and firm structure, considerable mechanical strength, wide speed range, and high operating efficiency, especially for high-speed and ultra-high-speed operation [7]–[10].

The motor in the flywheel battery needs to be used as a motor when storing energy and as a generator when releasing energy. Traditional motors can only operate independently in the electric or generating state, and an SRM can combine the functions of starter and generator because of its unique characteristics. When these two functions are realized in one motor, the number of devices used in the entire electrical system can be effectively reduced, and the volume of the entire electrical system is also reduced, reducing the cost [11]–[14].

To ensure stable operation of the SRM starting power generation system, timely maintenance and adjustment can ensure that the system will not produce major electrical faults. However, the selection of the period between maintenance times cannot be too small or too long, and so reliability analysis of the whole system is very important. Reliability research has a certain foundation at home and abroad. Traditional reliability calculation models usually include those of the reliability block diagram (RBD) [15], fault tree [16], *k*-out-of-*n*: G [17], [18] and Markov [19]–[21]. In general, the reliability block diagram and fault tree models are often used to calculate system-level reliability because of their simple structure and easy implementation [13], [14]. However, because an SRM has a strong fault-tolerant capability and that capability cannot be injected into the reliability model, these two models cannot be directly used for the reliability model calculation of an SRM system. In paper [19], the reliability of a grid-connected inverter and effective fault-tolerant topology is compared through a Markov

Received: February 15, 2023
Accepted: November 1, 2023
Published Online: January 1, 2024
Hao Chen (corresponding author), is with the School of Electrical Engineering, China University of Mining and Technology, Xuzhou 221116, China; with the Xinjiang Institute of Engineering, Urumqi 830000, China; with the International Joint Research Center of Central and Eastern European Countries on New Energy Electric Vehicle Technology and Equipment, Xuzhou 221008, China; and with the International Cooperation Joint Laboratory of New Energy Power Generation and Electric Vehicles of Jiangsu Province Colleges and Universities, Xuzhou 221008, China (e-mail: hchen@cumt.edu.cn).
DOI: 10.23919/PCMP.2023.000104

model, indicating that the proposed topology is a more reliable choice to improve performance. The Markov model is adopted in [20], [21] to evaluate the reliability of the motor driving system. In the system reliability evaluation, the Markov model can take the fault mode that can still operate as the operational state of the system. This method can improve the accuracy of system reliability evaluation, but the SRM starting power generation system includes three units: detection, motor prototype and power converter. At the same time, it is necessary to evaluate the reliability of the electrical mode and power generation mode simultaneously for the switched reluctance starter/generator system. Although the Markov model can be effectively used for reliability evaluation of the whole drive system, when the evaluation model is too complex, the low-order Markov model cannot evaluate the whole drive system accurately, and when the higher-order Markov model is applied, the large number of inevitable states will increase the complexity of the solution process and will cause some errors. The *k*-out-of-*n*: G model is a simple model and solution process, and can effectively obtain the impact of fault tolerance on reliability [17], [18]. In recent years, most research on the reliability of the SRM driving system has focused on the reliability analysis in the electric state, while there has been very little research on the reliability of the SRM starting power generation system. However, SRS/G is increasingly widely used, so it is particularly important to study the reliability of an SRS/G system. Therefore, this paper adopts the method of combining the RBD and *k*-out-of-*n*: G models to analyze the reliability of the starter/generator system. The evaluating method adopted here can not only accurately obtain the optimal maintenance time and improve the safety and reliability of the system, but also can reduce the complexity of the reliability mathematical model.

The rest of this article is structured as follows: the second part analyzes the electrical operational status and generating operational status of the SRM, and quantitatively analyzes the system operational status of the electrical and braking systems' fault operation using different fault criteria. In the third part, a *k*-out-of-*n*: G model state transition diagram of electric and power generation states is drawn. Finally, the system is evaluated and calculated by the selected reliability analysis method combining the *k*-out-of-*n*: G and RBD models.

II. Operating Characteristics of the SRM Starting Power Generation System

Traditional motors generally only need single-quadrant operation. As a motor, the energy is converted from electrical to mechanical. As a generator, the energy is converted from mechanical to electrical. The starting generator needs to have both the electrical and power generation states, so the reliability analysis of both those states is required.

A. Electrical Mode

Taking phase A as an example, the electrical mode mainly includes three types: excitation, zero voltage continuous current and negative voltage demagnetization states. The current path in the excitation state is shown in Fig.1 (a), and the voltage equation is:

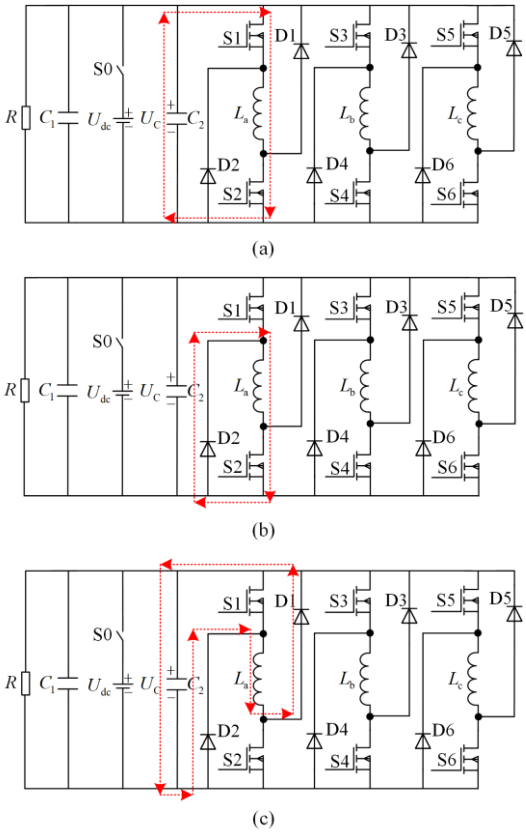

Fig. 1. Current path in the electrical mode. (a) Excitation state. (b) Zero voltage continuous current state. (c) Negative voltage continuous current state.

$$U_{dc} = iR + L\frac{di}{dt} + i\frac{dL}{d\theta} \tag{1}$$

where U_{dc} is the bus voltage; i, R and L are the current, resistance and inductance of each phase.

The current path in the zero-voltage freewheeling state is shown in Fig. 1(b), and the voltage equation is:

$$0 = iR + L\frac{di}{dt} + i\frac{dL}{d\theta} \tag{2}$$

The current path in the negative voltage demagnetization state is shown in Fig. 1(c), and the voltage equation is:

$$-U_{dc} = iR + L\frac{di}{dt} + i\frac{dL}{d\theta} \tag{3}$$

B. Power Generation Mode

For switched reluctance motors, in the electrical mode, the SRM conduction region is in the inductance rising region. At this time, the motor generates forward torque and electrical energy is converted to mechanical energy. In the SRG power generation mode, the conduction section is in the inductance drop area, at which time the

motor generates negative torque and the mechanical energy is converted to electrical energy. The relationship between the energy conversion and the position of the conduction section of the motor is shown in Table I. The torque formula of the motor is as follows:

TABLE I
ENERGY CONVERSION OF DIFFERENT POSITION

θ	Changing rate of inductance	Torque	Energy conversion
$0^\circ < \theta < 45^\circ$	+	+	Electric energy → Mechanical energy
$45^\circ < \theta < 90^\circ$	−	−	Mechanical energy → Electric energy

$$T_e = 0.5 i^2 \frac{\mathrm{d}L}{\mathrm{d}\theta} \tag{4}$$

It can be seen from the above formula that the positive and negative phase torque is only related to the changing rate of phase inductance. When the changing rate of inductance is positive, and the phase is conductive in this section, the phase torque generated is positive, and the energy of the motor is converted from electrical energy to mechanical energy. When the changing rate of inductance is negative, and the motor is conductive in this section, the phase torque generated is negative, and the energy of the motor is converted from mechanical energy to electrical energy. Since the motor used in this paper is a 6/4 motor, the inductance changing rate is negative when the rotor position is greater than 45° but less than 90°, and positive when the rotor position is greater than 0° but less than 45°. The relationship between inductance curve and rotor is shown in Fig. 2.

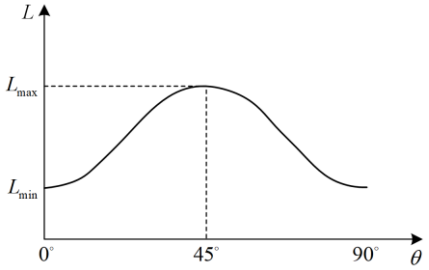

Fig. 2. Relationship between inductance and rotor.

III. ESTABLISHMENT OF RELIABILITY SYSTEM FOR AN SRM STARTING POWER GENERATION SYSTEM

A. Failure Mode

The switched reluctance starting/generating system consists of three parts: power converter, motor prototype and detection unit. Because of the strong fault tolerance of a switched reluctance motor, it is necessary to inject different fault modes into the reliability model to obtain accurate results. Failure modes can be summarized as three parts.

For the motor prototype, the fault mode is mainly divided into two cases: open circuit (OW) and short circuit (SW) on the winding.

For power converters, fault modes mainly include 10 types of circuit: capacitor open (OC), capacitor short (SC), upper diode open (OUD), upper diode short (SUD), lower diode open (OLD), lower diode short (SLD), upper MOSFET open (OUM), upper MOSFET short (SUM), lower MOSFET open (OLM), and lower MOSFET short (SLM).

The detection unit is a rotary encoder (position sensor) and current sensor. Therefore, for the detection part, the fault mode mainly includes five cases: position sensor no output (OPS), position sensor constant output (CPS), current sensor no output (OCS), current sensor gain output (GCS), and current sensor constant output (CCS) [22]–[24].

B. Fault Criteria

After the failure mode is introduced, it is necessary to determine whether the system can still operate stably after the failure occurs. Therefore, this paper proposes a fault criterion suitable for determining the operational state of the system. In the SRM starting and generating system, the fault criteria of the electrical and generating states are different.

In this paper, in the electric mode, the speed n is the embodiment of the system stability, so the speed fluctuation k can be used to describe the system stability.

$$k = \frac{n_{max} - n_{min}}{n_{ref}} \tag{5}$$

where n_{max} is the maximum speed of the system in stable operation; n_{min} is the minimum speed of the system in stable operation; and n_{ref} is the reference speed. When the system operates normally, k is equal to 1. When the system fails, k also changes. In this paper, when the value of k exceeds 10%, the system is deemed to be in a fault state. At the same time, the safe operation of the system is also a very important part, so when the peak phase current i_{ph} exceeds 40 A, the system is also considered as in fault.

In the power generation mode, the power generation efficiency of the system is used as a criterion to judge whether the system is in a fault state. The generating power of the system is expressed by the following formula:

$$P_{tot} = \frac{1}{T_{ph}} \left(\int_0^{T_{ph}} i_a u_a \mathrm{d}t + \int_0^{T_{ph}} i_b u_b \mathrm{d}t + \int_0^{T_{ph}} i_c u_c \mathrm{d}t \right) \tag{6}$$

where i_a, i_b, i_c is the phase current of each phase; and u_a, u_b, u_c is the phase voltage of each phase.

The ratio m of the generated power in fault conditions and the generated power in normal conditions is used as the fault standard in the generation mode. When the value of m is less than 0.4, the switched reluctance motor starting power generation system is deemed to be invalid. At the same time, when the peak current exceeds 80 A, the system is deemed as invalid.

$$m = \frac{P_{\text{tot\_F}}}{P_{\text{tot\_N}}} \tag{7}$$

C. Reliability Model

For an SRM starting power generation system, the reliability of electrical and power generation modes needs to be calculated, and the reliability of the system can be expressed as:

$$R(t)_{\text{sys}} = R(t)_{\text{dri}} R(t)_{\text{gen}} \tag{8}$$

where $R(t)_{\text{sys}}$ represents the reliability of the whole system, $R(t)_{\text{dri}}$ represents the reliability in the electrical state, and $R(t)_{\text{gen}}$ represents the reliability in the power generation state.

The RBD model of the system is the same for the generating and electrical states, as shown in Fig. 3. However, the reliability calculations for the power generation and electrical states need to be calculated separately.

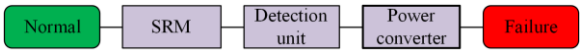

Fig. 3. RBD model of the system.

$$R(t)_{\text{dri}} = R(t)_{\text{SRM\_d}} R(t)_{\text{det\_d}} R(t)_{\text{pow\_d}} \tag{9}$$

$$R(t)_{\text{gen}} = R(t)_{\text{SRM\_g}} R(t)_{\text{det\_g}} R(t)_{\text{pow\_g}} \tag{10}$$

where $R(t)_{\text{SRM\_d}}$ is the reliability of the motor body in the electrical mode; $R(t)_{\text{det\_g}}$ is the reliability of the detection unit in electrical mode; $R(t)_{\text{pow\_d}}$ is the reliability of power converter in electrical mode; $R(t)_{\text{SRM\_g}}$ is the reliability of the motor body in the power generation mode; $R(t)_{\text{det\_g}}$ is the reliability of the detection unit in the power generation mode; $R(t)_{\text{det\_g}}$ is the reliability of the power converter in the power generation mode. To obtain the reliability of the switched reluctance generator more accurately, we compare the reliability evaluation using the Markov model with that using the *k*-out-of-*n*: G model.

1) First-order Markov Model

When the first-order Markov model determines that the system has two or more faults, the system is deemed to be failed. The failure rate of the device can be obtained through the manual MIL-HDBK-217F [25]. It is worth mentioning that when the second-order Markov model is used to calculate the reliability of the system, the calculation formula is too complex, and thus the second-order Markov model will not be used to analyze the reliability model of the system in this paper.

The device failure rate can be calculated as [25]:

$$\lambda_{\text{p}} = \lambda_{\text{b}} \pi_{\text{A}} \pi_{\text{Q}} \pi_{\text{E}} \pi_{\text{S}} \pi_{\text{T}} FP \tag{11}$$

where the basic failure rate is λ_{b}; the applied stress is expressed as π_{A}; the mass stress as π_{Q}; the environmental stress as π_{E}; the electrical stress as π_{S}, the temperature stress as π_{T}; and the failure probability is expressed as *FP*. Then, the value of failure rate can be expressed quantitatively in Table II, where the symbol λ_{XX} represents the failure rate under XX failure. For example, λ_{SC} is the failure rate of a capacitor in the case of a short circuit fault. When calculating the failure rate, the ambient temperature is set at 30°C. The fault symbols in the Markov state transition diagram are shown in Table III. The Markov transfer diagram of starting generator components is shown in Fig. 4.

TABLE II
DEVICE FAILURE RATE

Fault type	Failure rate (10^{-6}h)	Fault type	Failure rate (10^{-6}h)
λ_{SC}	0.4854	λ_{SLM}	2.4255
λ_{OUD}	0.2409	λ_{SM}	0.3840
λ_{SUD}	0.4236	λ_{OC}	0.3205
λ_{OLD}	0.2409	λ_{OW}	0.3840
λ_{SLD}	0.4236	λ_{OUM}	1.5219
λ_{SUM}	2.4255	λ_{OLM}	1.5219

TABLE III
FAULT STATE SYMBOLS OF FIRST-ORDER MARKOV TRANSITION DIAGRAM

Symbol	State	Symbol	State
A1	OW	A2	SW
A3	failure	A4	GCS
A5	failure	A6	OC
A7	OUM	A8	OLM
A9	SLM	A10	failure
A11	SUM	A12	failure

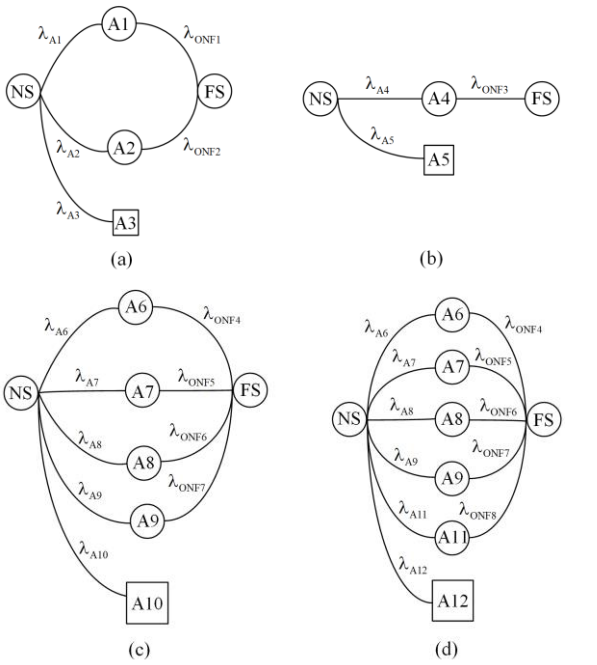

Fig. 4. First-order Markov model. (a) SRM body. (b) Detection unit. (c) Power converter in electric state. (d) Power converter in power generation state.

Using the first-order Markov model reliability calculation, we can get:

$$R_1 = (-13.018e^{-28.3124t} + e^{-27.9919t} + 7.018e^{-26.7905t} + 6e^{-25.8869t}) \times (-10.018e^{-28.3124t} + e^{-27.9919t} + 7.018e^{-26.7905t} + 3e^{-25.8869t}) \times (6e^{-1.92t} - 5e^{-2.304t})^{\wedge 2} \times (-2e^{-3.59t} + 3e^{-3.46t})^{\wedge 2} \quad (12)$$

2) k-out-of-n: G Model

In the *k*-out-of-*n*: G model, the system is considered to be invalid unless at least *k* components work normally [26]. As shown in Fig. 5, the *k*-out-of-*n*: G model can be calculated by the following formula:

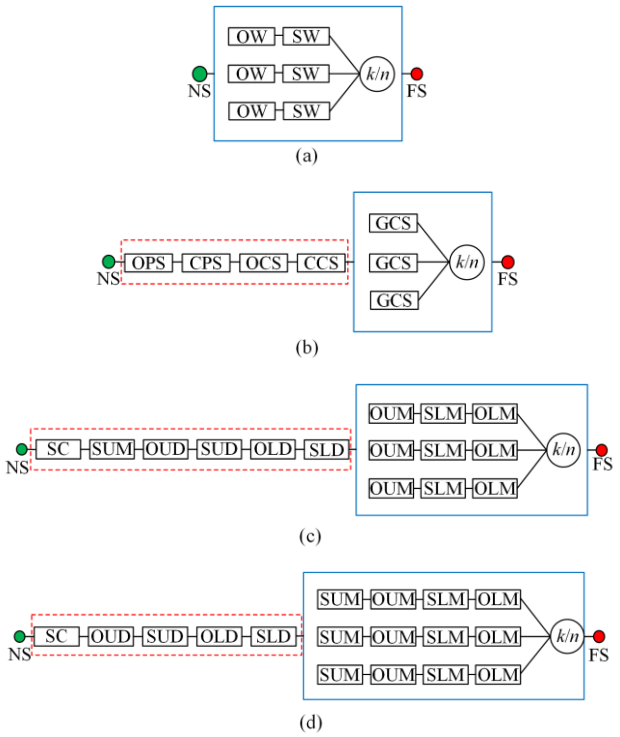

Fig. 5. *k*-out-of-*n*: G model. (a) SRM prototype. (b) Detection unit. (c) Power converter in electric state. (d) Power converter in power generation state.

$$R_K(t) = e^{-\lambda_1 t} \times \left[\sum_k^n e^{-k\lambda_2 t} \times (1 - e^{-\lambda_2 t})^{n-k} \right] \quad (13)$$

where λ_1 is the sum λ values in the red box; λ_2 is the sum λ values of the single line in the blue box. Then the reliability calculation of the system using the *k*-out-of-*n*: G model is:

$$R_2(t) = e^{-50.8516t} \quad (14)$$

The safe operational life of the system can be expressed as:

$$MTTF = \int_0^\infty R(t)\mathrm{d}t \quad (15)$$

From the above formula, the reliability life of the system is calculated as shown in Table IV.

As is shown in Table IV, the reliability life of the *k*-out-of-*n*: G model is 19665 hours and the reliability life of the Markov model is 18835 hours. This means that the useful life of the *k*-out-of-*n*: G model is similar to that of the Markov model. However, equation (12) is too complex when it is expanded. In other words, the Markov model is more prone to errors in calculation.

TABLE IV
RELIABILITY CALCULATION

Model	Markov	*k*-out-of-*n*:G
Reliability life (h)	18 835	19 665

IV. SIMULATION AND EXPERIMENTAL VERIFICATION

The prototype selected in this paper is a three-phase 6/4 SRM. The geometric parameters of the motor are shown in Table V.

TABLE V
GEOMETRIC PARAMETERS OF PROTOTYPE

Parameter	size	Parameter	size
Outer diameter of stator D_s	122.5 mm	Thickness of rotor yoke h_{ry}	11.00 mm
Thickness of stator yoke h_{sy}	11.00 mm	Rotor pole arc angle β_r	34.69°
Stator pole arc angle β_s	32.88°	Shaft diameter D_{sh}	20.00 mm
air gap δ	0.30 mm	Laminate thickness L_{stk}	70.00 mm
Outer diameter of rotor D_r	62.5 mm	Winding turns per phase N	72

A. Simulation Verification

1) Electrical Mode

In the electrical mode, the current and speed waveforms during the normal operation of the system are shown in Fig.6. During operation, when only phase A has an OUM fault, i_A decreases to 0, i_B and i_C increase slightly, but the system speed is basically unchanged, and the speed fluctuation *k* is not more than 10%, as shown in Fig. 7. Therefore, when the OUM fault occurs

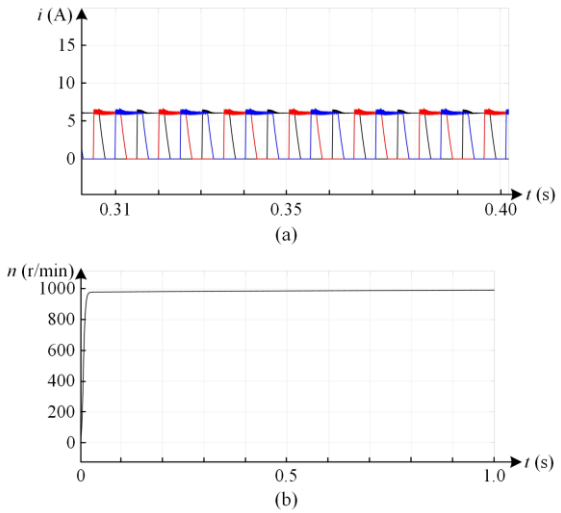

Fig. 6. Simulated current and speed waveform in electrical mode: normal state. (a) Current. (b) Speed.

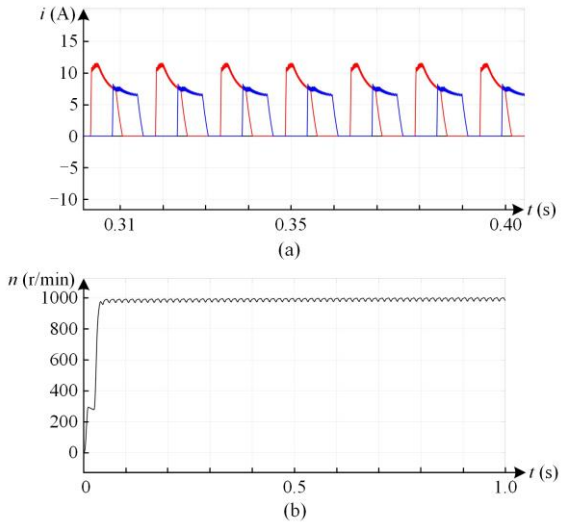

Fig. 7. Simulated current and speed waveform in electrical mode: OUM fault. (a) Current. (b) Speed.

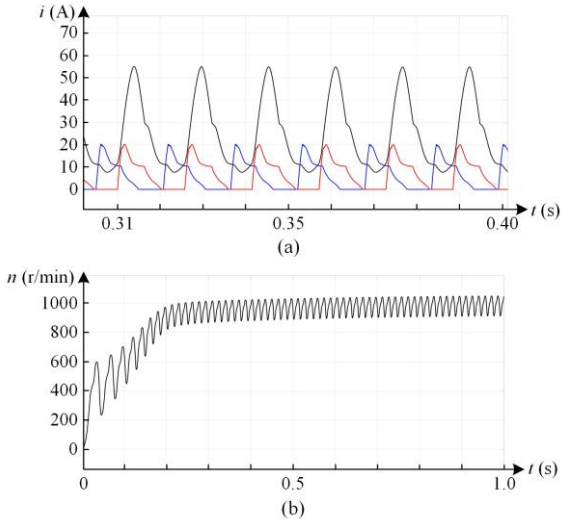

Fig. 8. Simulated current and speed waveform in electric mode: SLM fault. (a) Current. (b) Speed.

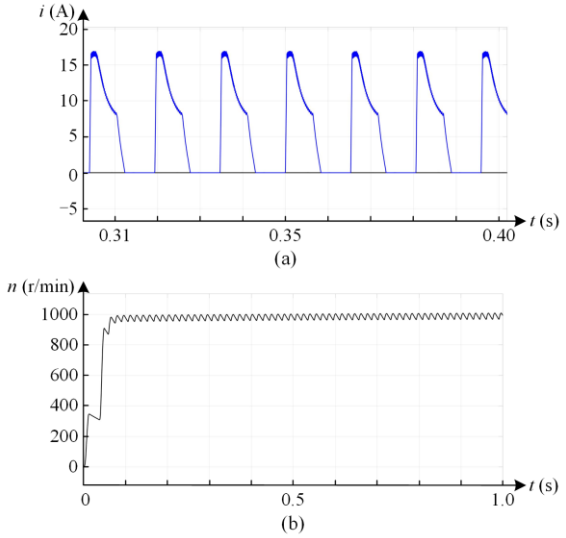

Fig. 9. Simulated current and speed waveform in electrical mode: two-phase OUM fault. (a) Current. (b) Speed.

in phase A, the system is determined to be operating safely. When an SUM fault occurs in phase A, i_A exceeds the recognized safe current of 40 A, so the system is considered to be in a fault state, as shown in Fig. 8. As shown in Fig. 9, when both phase A and phase B have an OUM fault, i_A and i_B are both 0, and i_C rises to 17 A to maintain the system running at a speed of 1000 r/min. The speed fluctuation k is not more than 10%, so the system is considered to be in safe operation.

2) Power Generation Mode

In the power generation mode, the current during the normal operation of the system is shown in Fig. 10(a). When the OUM fault occurs in phase A, as shown in Fig. 10(b), i_A decreases to 0, i_B and i_C remain unchanged, and the index m in the power generation mode still exceeds 0.4. Therefore, when the OUM fault occurs in phase A, the system is determined to be operating safely. When an SUM fault occurs in phase A, as shown in Fig. 10(c), i_A rises but does not exceed 80 A, and the

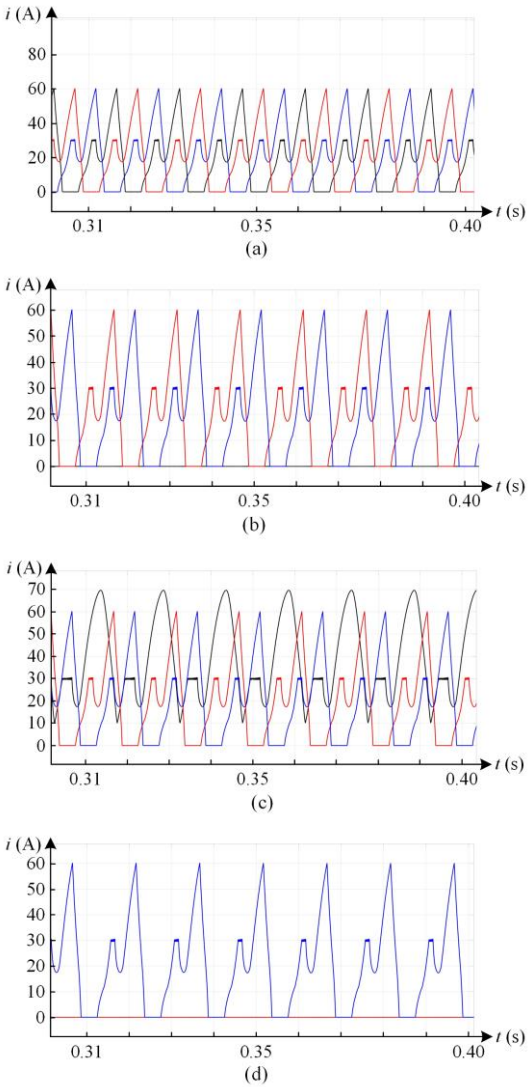

Fig. 10. Simulated current waveform under power generation mode. (a) Normal state. (b) OUM fault. (c) SUM fault. (d) Two-phase OUM fault.

system is considered as in a failure state. As shown in Fig. 10(d), when both phase A and phase B have an OUM fault, i_A and i_B fall to 0, and the index m in the power generation mode is less than 0.4, the system is considered to be in a fault state.

B. Experimental Verification

1) Experimental Platform

In order to verify the correctness of the established reliability model, an SRG experimental platform was built, as shown in Fig. 11. The SRG is driven by the asynchronous motor to reach the specified speed. The power converter adopts a three-phase asymmetrical half-bridge, the excitation mode adopts a separate excitation mode, and the excitation voltage is 48 V.

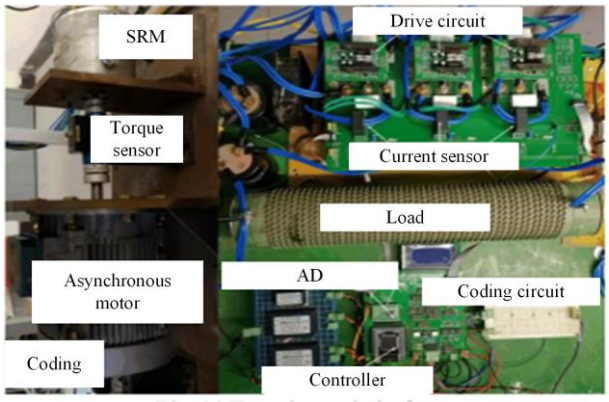

Fig. 11. Experimental platform.

2) Electrical Mode

The experiment uses a 6/4 structure three-phase switched reluctance motor. Fig. 12(a) shows the three-phase current in electrical mode when the motor has no fault at 1000 r/min. Comparing with Fig. 7, the simulation and experimental results are very similar.

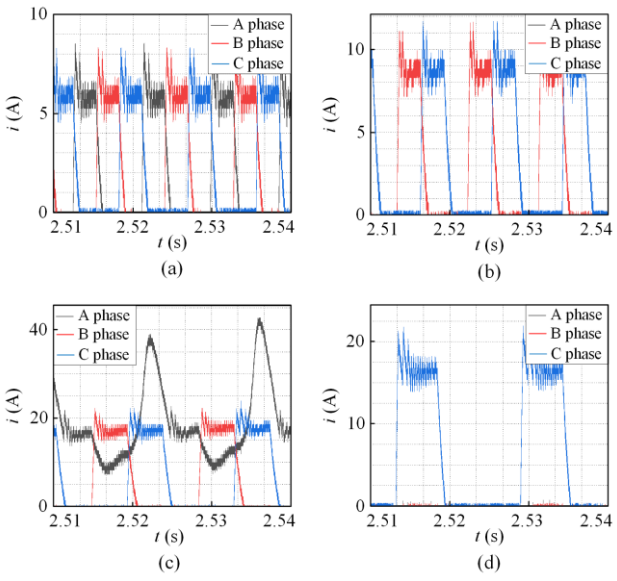

Fig. 12. Current waveform of the test in electric mode. (a) Normal state. (b) OUM fault. (c) SUM fault. (d) Two-phase OUM fault.

Figure 12(b) shows the three-phase current of the system after the OUM fault of phase A. The phase A current changes to 0, and the phase B and C current increases from 6 A to 10 A to maintain the speed at 1000 r/min. From the fault criteria in the drive mode, the system is still in safe operation at this time. Figure 12(c) shows the three-phase current of the system when the SUM fault occurs in phase A. The phase A current exceeds the safety current peak value of 40 A, so the system is considered as in fault. Figure 12(d) shows the three-phase current of the system when the OUM fault occurs in both phase A and phase B. At this time, the current of phase A and B drops to 0, and the current of phase C rises to 15–20 A. According to the fault criteria in the electrical mode, the system is considered to operate in a safe state at this time.

3) Power Generation Mode

In the power generation mode, the three-phase current waveform of the motor without fault at 1000 r/min is shown in Fig. 13(a). Figure 13(b) shows the three-phase current after the OUM fault of phase A in the system. The phase A current drops to 0, and the phase B and C current do not change. With reference to the fault standard in the power generation mode, the system is deemed to be in safe operation. Figure 13(c) shows the three-phase current of the system when the SUM fault occurs in phase A. Since the one-phase current exceeds the safe peak current of the system by 80 A, the system is considered as being in fault. Figure 13(d) shows the three-phase current of the system when both phase A and phase B have an OUM fault. Phase A and phase B current are zero, and phase C current is unchanged, but the system power generation capacity is only 1/3 of the normal state, which is lower than the safe operation value of 0.4, which is considered as a fault.

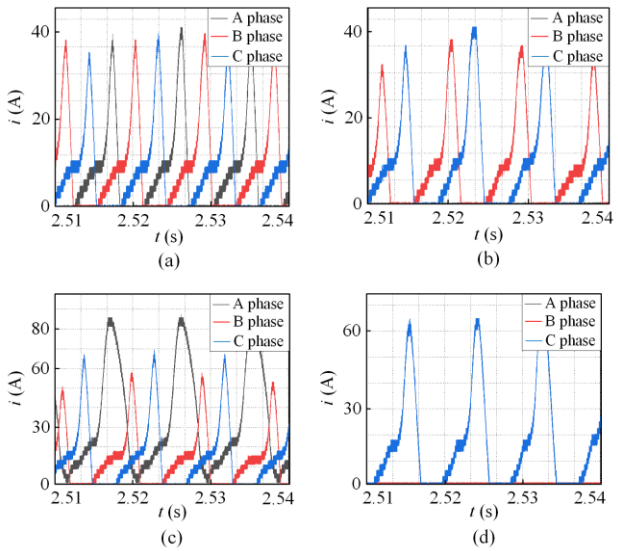

Fig. 13. Current waveform of the test under power generation mode. (a) Normal state. (b) OUM fault. (c) SUM fault. (d) Two-phase OUM fault.

V. Conclusion

In this paper, a reliability analysis method considering both electrical and power generation mode is proposed, and the reliability of an SRS/G system is analyzed. To reduce the complexity of the mathematical model of the whole system, the system-level reliability RBD model is adopted. To reflect the fault tolerance of the switched reluctance motor, the reliability evaluation of the motor type, the detection unit and the power converter using a Markov model and a *k*-out-of-*n*: G model are compared. The results show that the *k*-out-of-*n*: G model reduces the complexity of the algorithm and improves the accuracy of reliability analysis. Different from the traditional reliability analysis model, different failure criteria for starting and generating modes are put forward in this paper, and then the operational status of the system under different failure criteria are analyzed. The reliability analysis method proposed can intuitively describe the fault-tolerant performance of the system, and can more accurately describe the operating state of the system. This method also fills the gap of reliability analysis of a switched reluctance starting/generating system.

Acknowledgment

Not applicable.

Author's Contributions

Hao Chen: full-text writing and innovative points proposing. Fan Yang: software and simulations. Lijun Xu: English improvement and construction of the paper framework. Qiwei Lu: experimental guidance. Xiqiang Chang: format adjustment. Xing Wang: experimental assistance. Lijiang Dong: English improvement. Yi Wen: guidance on article structure. Jiang Chen: English improvement. Gang Miao: improvement of experimental methods. Jianmin Hu: simulation guidance. Guanjun Wang: article structure adjustment. Wei Li: literatures review. Xiaohua Bao: English improvement. All authors read and approved the final manuscript.

Funding

This work is supported in part by the Jiangsu Science and Technology Plan Special Fund (Innovation Support Plan International Science and Technology Cooperation/ Hong Kong Macao Taiwan Science and Technology Cooperation Project (No. BZ2022014), the Cooperation and Exchange Program between NSFC and RS (No. 52211530083), and the Shenzhen International Science and Technology Independent Cooperation Project and Key R&D projects in Xinjiang Uygur Autonomous Region (No. 2022B01003-1).

Availability of Data and Materials

Not applicable.

Declarations

Competing interests: The authors declare that they have no known competing financial interests or personal relationships that could have appeared to influence the work reported in this article.

Authors' Information

Hao Chen received B.S. and Ph.D. degrees in electrical engineering from the Department of Automatic Control, Nanjing University of Aeronautics and Astronautics, Nanjing, China, in 1991 and 1996, respectively. In 1998, he became an Associate Professor with the School of Information and Electrical Engineering, China University of Mining and Technology, Xuzhou, China, where he has been a Professor since 2001. From 2002 to 2003, he was a Visiting Professor at Kyungsung University, Busan, Korea. Since 2008, he has also been an Adjunct Professor at the University of Western Australia, Perth, Australia. He is the author of one book and has also authored more than 200 papers. He is the holder of 15 US Patents, 23 Australian Patents, 1 Danish Patent, 7 Canadian Patents, 3 South African Patents, 10 Russian Patents, 76 Chinese Invention Patents and 6 Chinese Utility Model Patents. His current research interests include motor control, linear launcher, electric vehicles, electric traction, servo drives, and wind power generator control.

Fan Yang received his B.S. degree from the Yancheng Institute of Technology, Yancheng, China, in 2012. He is presently working towards his Ph.D. degree in the School of Information and Electrical Engineering, China University of Mining and Technology, Xuzhou, China. His current research interests include reliability analysis and direct torque control strategies.

Lijun Xu received his Ph.D. degree from Xinjiang University in Power System and Automation. Now he is the professor of Xinjiang Institute of Engineering, Urumqi, China.

Qiwei Lu received his B.S. degree and Ph.D. degree from China University of Mining and Technology (Beijing) in Power Electronics and Power Transmission. Now he is the professor of China University of Mining and Technology (Beijing), Beijing, China.

Xiqiang Chang now is working at State Grid Xingjiang Electric Power Co., Ltd., Urumqi, Xinjiang, China.

Xing Wang received her B.S. degree from China University of Mining and Technology in Computer Science

and Technology and received her Master's degree from China University of Mining and Technology in Management Engineering. Now she is the associate professor of China University of Mining and Technology, Xuzhou, China.

Lijiang Dong now is working at State Grid Xinjiang Company Limited Electric Power Research Institute, Urumqi, Xinjiang, China.

Yi Wen now is working at Xinjiang Fukang Pumped Storage Power Company Limited, Urumqi, Xinjiang, China.

Jiang Chen now is working at State Grid Urumqi Electric Power Supply Company, Urumqi, Xinjiang, China.

Gang Miao now is working at State Grid Urumqi Electric Power Supply Company, Urumqi, Xinjiang, China.

Jianmin Hu now is working at State Grid Urumqi Electric Power Supply Company, Urumqi, Xinjiang, China.

Guanjun Wang now is working at Wuxi Inspection and Testing Certification Research Institute, Wuxi, Jiangsu, China.

Wei Li now is working at Anhui Wannan Electric Machine Co., Ltd., Wannan, Anhui, China.

Xiaohua Bao received his B.S. degree and Ph.D. degree from Hefei University of Technology, Hefei, Anhui, China. Now he is the professor of Hefei University of Technology in Electrical and Automation Engineering.

REFERENCES

[1] S. Liu, C. Zhou, and H. Guo *et al*., "Operational optimization of a building-level integrated energy system considering additional potential benefits of energy storage," *Protection and Control of Modern Power Systems*, vol. 6, no. 1, pp. 55-64, Jan. 2021.

[2] O. J. Olujobi, "The legal sustainability of energy substitution in Nigeria's electric power sector: renewable energy as alternative," *Protection and Control of Modern Power Systems*, vol. 5, no. 4, pp. 358-369, Oct. 2020.

[3] X. WANG, J. GE, and L. HAN *et al*., "Theory and practice of grid-forming BESS supporting the construction of a new type of power system," *Power System Protection and Control*, vol. 51, no. 5, pp. 172-179, Mar. 2023. (in Chinese)

[4] Z. CHU, L. ZHAO, and J. SUN *et al*., "Thermoelectric optimization of an integrated energy system with hydrogen energy storage considering thermal energy dynamic balance," *Power System Protection and Control*, vol. 51, no. 3, pp. 1-12, Feb. 2023. (in Chinese)

[5] S. Koohi-Fayegh and M. Rosen, "A review of energy storage types, applications and recent developments," *Journal of Energy Storage*, vol. 7, no. 1, pp. 1323-1333, Jan. 2020.

[6] Y. Mi, B. Chen, and P. Cai, *et al*., "Frequency control of a wind-diesel system based on hybrid energy storage," *Protection and Control of Modern Power Systems*, vol. 7, no. 3, pp. 446-458, Jul. 2022.

[7] I. Husain, "Minimization of torque ripple in SRM drives," *IEEE Transactions on Industrial Electronics*, vol. 49, no. 1, pp. 28-39, Jan. 2002.

[8] I. Ralev, F. Qi, and B. Burkhart *et al*., "Impact of smooth torque control on the efficiency of a high-speed automotive switched reluctance drive," *IEEE Transactions on Industrial Application*, vol. 53, no. 1, pp. 5509-5517, Jan. 2017.

[9] S. Sahoo, S.Panda, and J. Xu, "Indirect torque control of switched reluctance motors using iterative learning control," *IEEE Transactions on Power Electronics*, vol. 20, no. 1, pp. 200-208, Jan. 2005.

[10] A. Xu, C. Shang, and J. Chen *et al*., "A new control method based on DTC and MPC to reduce torque ripple in SRM," *IEEE Access*, vol. 7, no. 1, pp. 68584-68593, Jan. 2019.

[11] S. Yao, and W. Zhang, "A simple strategy for parameters identification of SRM direct instantaneous torque control," *IEEE Transactions on Power Electronics*, vol. 33, no. 4, pp. 3622-3630, Apr. 2018.

[12] B. Deng, H. Mecrow, and R. Martin, "Design and development of low torque ripple variable-speed drive system with six-phase switched reluctance motors," *IEEE Transactions on Energy Conversion*, vol. 33, no. 1, pp. 420-429, Jan. 2018.

[13] H. Chen, H. Chen, and G. Han *et al*., "Power transistors' fault diagnosis method of SR S/G for more electric aircraft with cross-leg current analysis," *IEEE Transactions on Transportation Electrification*, vol. 6, no. 4, pp. 1528-1536, Dec. 2020.

[14] H. Chen, G. Guan, and G. Han *et al*., "Fault diagnosis and tolerant control strategy for position sensors of switched reluctance starter/generator systems," *IEEE Transactions on Transportation Electrification*, vol. 6, no. 4, pp. 1508-1518, Dec. 2020.

[15] R. Burgos, G. Chen, and F. Wang *et al*., "Reliability-oriented design of three-phase power converters for aircraft applications," *IEEE Transactions on Aerospace and Electronic Systems*, vol. 48, no. 2, pp. 1249-1263, Apr. 2012.

[16] F. Chan and H. Calleja, "Design strategy to optimize the reliability of grid-connected PV systems,". *IEEE Transactions on Industry Electronics*, vol. 56, no. 11, pp. 4465-4472, Nov. 2009.

[17] F. Richardeau and T. Pham, "Reliability calculation of multilevel converters: theory and applications,"

IEEE Transactions on Industrial Electronics, vol. 60, no. 10, pp. 4225-4233, Oct. 2013.

[18] H. Chen, H. Yang, and Y. Chen et al., "Reliability assessment of the switched reluctance motor drive under single switch chopping strategy," *IEEE Transactions on Power Electronics*, vol. 31, no. 3, pp. 2395-2408, Mar. 2016.

[19] W. Li and M. Cheng, "Reliability analysis and evaluation for flux-switching permanent magnet machine," *IEEE Transactions on Industrial Electronics*, vol. 66, no. 3, pp. 1760-1769, Mar. 2019.

[20] F. Richardeau and T. Pham, "Reliability calculation of multilevel converters: theory and applications," *IEEE Transactions on Industrial Electronics*, vol. 60, no. 10, pp. 4225-4233, Oct. 2013.

[21] P. Tu, S. Yang, and P. Wang, "Reliability- and cost-based redundancy design for modular multilevel converter," *IEEE Transactions on Industrial Electronics*, vol. 66, no. 3, pp. 2333-2342, Mar. 2019.

[22] H. Chen, H. Yang, and Y. Chen *et al*., "Reliability assessment of the switched reluctance motor drive under single switch chopping strategy," *IEEE Transactions on Power Electronics*, vol. 31, no. 3, pp. 2395-2408, Mar. 2016.

[23] S. Xu, H. Chen, and F. Dong *et al*., "Reliability analysis on power converter of switched reluctance machine system under different control strategies," *IEEE Transactions on Industrial Electronics*, vol. 66, no. 8, pp. 6570-6580. Aug. 2019.

[24] H. Chen, S. Xu, and W. Wei, "Reliability assessment of double-sided linear switched reluctance generator system based on hierarchical Markov model," *IEEE Transactions on Industrial Electronics*, vol. 66, no. 6, pp. 4901-4911, Jun. 2019.

[25] M. J. Leish, "Enhancing MIL-HDBK-217 reliability predictions with physics of failure methods," in *2010 Proceedings-Annual Reliability and Maintainability Symposium (RAMS)*, San Jose, USA, Jan. 2010, pp. 1-6.

[26] F. Richardeau and T. Pham, "Reliability calculation of multilevel converters: theory and applications," *IEEE Transactions on Industrial Electronics*, vol. 60, no. 6, pp. 4225-4233, Jun. 2013.